DOI: 10.1002/anie.200906439

O_2 Evolution

Evolution of O_2 in a Seven-Coordinate Ru^{IV} Dimer Complex with a $[HOHOH]^-$ Bridge: A Computational Study**

*Jonas Nyhlén, Lele Duan, Björn Åkermark, Licheng Sun, and Timofei Privalov**

Catalytic water oxidation is an essential part of light-driven splitting of water into H_2 and O_2.[1–8] This process would be a clean, renewable and sustainable solution to the energy demands of humanity.[9] Despite many efforts, the features critical for efficient catalytic water oxidation, are insufficiently understood. A major reason is the difficulty of characterizing the reaction intermediates, which are unstable, presumably because of the presence of high-valent metal centers. Continued efforts to understand the reaction mechanism and to find more efficient and robust catalysts are therefore essential.[10–21]

Although over the years, six-coordinate dinuclear ruthenium centers have been the staple of mechanistic rationale for a number of reported water oxidation catalysts,[10–16,19–21] involvement of seven-coordinate mononuclear intermediates has recently been considered.[10a,14]

A few months ago, we discovered a new water-oxidation catalyst, the Ru^{II} complex **1** (Figure 1). The kinetics of catalytic water oxidation were second order in complex **1**, suggesting that the reaction proceeds via a dimeric complex, such as **2** (Figure 1).[21] In fact, both complex **1** and the uncommon seven-coordinate dimeric Ru^{IV} complex **2**, were isolated and structurally characterized by X-ray crystallography.[21] The novel structural aspects of complex **1** and the experimentally verified involvement of seven-coordinate ruthenium dimer (**2**) in the catalytic water oxidation raise the following key questions: What are coordination geometries of the Ru centers in different oxidation states? What are the redox properties? What is the role of the hydrogen-bonding network? In view of the uncommon seven-coordinate Ru centers in complex **2**, what is a plausible mechanism of O_2 evolution? Our study proposes answers to these and other central questions based on accurate calculations with hybrid density functional B3LYP within self-consistent reaction field (SCRF) solvent model.[22] Most importantly, we demonstrate that O_2 evolution via the direct interaction of oxygen radicals in the doubly oxidized dimer **2** and the subsequent redox-coupled release of O_2 does not require crossing of prohibitively high potential-energy barriers. We also uncover key electronic and structural aspects of seven-coordinate Ru centers.

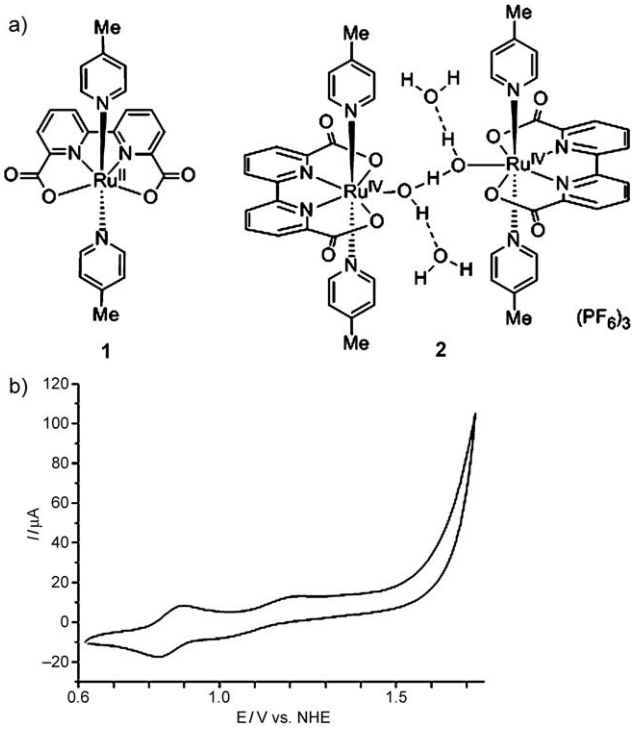

Figure 1. a) Molecular structures of $[Ru^{II}L(pic)_2]$ (**1**) (H_2L = 2,2′-bipyridine-6,6′-dicarboxylic acid; pic = 4-picoline) and [μ-(HOHOH)-{$Ru^{IV}L(pic)_2$}$_2$]$(PF_6)_3 \cdot 2H_2O$ (**2**) complexes based on crystal-structure determination. b) Cyclic voltammogram of **1** (1.0 mM) in CF_3SO_3H aqueous solution (pH 1.0) containing 10% acetonitrile.

The starting point of our study is complex **1** in aqueous solution. For all calculations, picoline groups are replaced by pyridine groups (py) for purely computational reasons. According to previously published methodology,[23] the standard Gibbs free energy of the redox half reaction contains the free energy difference of the redox pair in the gas phase and the difference in free energy of solvation of oxidized and reduced species as computed in SCRF calculations (the so-called Born–Haber cycle; details in the Supporting Information). All reported potentials are referenced to the normal hydrogen electrode (NHE).[24] To model proton-coupled redox reactions,[25] we employ the combination of SCRF with a dielectric constant of $\varepsilon = 80.37$ (water) and an explicit water dimer, $[H_4O_2]$, for the quantum mechanical portrayal of the solvated proton, $H^+[H_4O_2]$. This time-effective computa-

[*] J. Nyhlén, Prof. B. Åkermark, Prof. T. Privalov
Department of Chemistry, Arrhenius Laboratory
Stockholm University, 10691 Stockholm (Sweden)
E-mail: priti@organ.su.se
L. Duan, Prof. L. Sun
Department of Chemistry
School of Chemical Science and Engineering
Royal Institute of Technology (KTH), 10044 Stockholm (Sweden)

[**] We thank the Swedish Research Council, K & A Wallenberg Foundation, and the Swedish Energy Agency for financial support of this work.

Supporting information for this article is available on the WWW under http://dx.doi.org/10.1002/anie.200906439.

 © 2010 Wiley-VCH Verlag GmbH & Co. KGaA, Weinheim

tional method should be sufficiently accurate for our purposes.[26]

Electronic structure calculations of $[(H_2O)Ru(n+2)L(py)_2]^{n+}$ monomers **1**, where $n=0$, 1, 2, and 3, with the equilibrated explicit waters, were carried out at the B3LYP/lacvp** level of theory. Final structures are shown in Figure 2. The O-Ru-O angles are 167.8°, 158.7°, 150.1° and 146.5° in $\mathbf{1'}^{(n+)}$, $n=0$, 1, 2, 3, respectively. It is worth noting that the Ru^{II} d^6 center in **1′** (Figure 2) accommodates a water molecule at a seventh coordination site. The complex (**1′**) does so at the expense of the axial Ru–N bonds, which are significantly elongated relative to those in the gas-phase structure of **1** (Figure S1 in the Supporting Information).

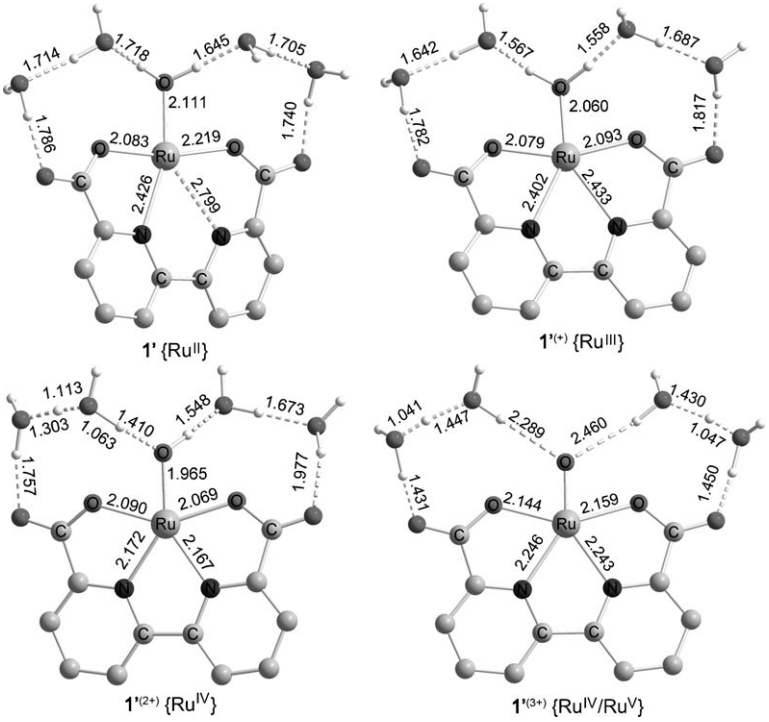

Figure 2. Calculated structures resulting from redox events in $[(H_2O)Ru(n+2)L(py)_2]^{(+n)}$ complexes, ($n=0$, 1, 2, and 3). The ruthenium-bound pyridine groups and hydrogen atoms except the HO type are omitted for clarity. All distances are in Å.

According to our calculations, 1) the one-electron transition from the **1′** (singlet) to the $\mathbf{1'}^{(+)}$ (doublet) occurs at 0.42 V; 2) at 0.92 V, the proton-coupled Ru^{III}/Ru^{IV} process affords aqueous $\{Ru^{IV}OH^{(-)} + H_3O^{(+)}\}$ complex ($\mathbf{1'}^{(2+)}$); 3) at 1.57 V, the proton-coupled oxidation of the Ru^{IV} complex ($\mathbf{1'}^{(2+)}$) affords formally the Ru^{V}=O complex ($\mathbf{1'}^{(3+)}$). Regarding the Ru^{V}=O complex, its ground state is in fact closer to that of a Ru^{IV} oxyl species: Mulliken spin populations of the Ru and O atoms are 0.3 and 0.7, in agreement with results obtained for metal oxyl radicals.[17,27] Whereas the Ru^{II}/Ru^{III} and Ru^{III}/Ru^{IV} processes occur at the metal atom, the oxidation beyond Ru^{IV} affords an oxyl complex (Figure 2). All the calculated redox potentials are in agreement with cyclic voltammogram of **1** in aqueous solution (pH 1.0) shown in Figure 1;[28] all the experimental details are reported in the Supporting Information.

We optimized **2** in an aqueous solvent. Although only two water molecules, hydrogen bonded to the $[HOHOH]^-$ group and the carboxylate groups, are present in the solid state of **2**, it is expected that in aqueous solution a complex hydrogen-bonding network will be formed. The result of the search for an optimal solvated structure ($\mathbf{2'}^{(3+)}$) is shown in Figure 3. We have found that the ground state of $\mathbf{2'}^{(3+)}$ is the closed-shell singlet for the $\{L(py)_2Ru^{IV}OH\text{-}O(H)Ru^{IV}L(py)_2\}^{3+}$ complex, which is a direct analogue of **2** without counterions. The loss of the proton, H1 in $\mathbf{2'}^{(3+)}$ (Figure 3), by Ru1-bound H_2O unit to the solvent environment is consistent with our results for $\mathbf{1'}^{(2+)}$. The alignment of the key hydrogen bond, the O1-H3-O2 bridging fragment between the Ru centers in $\mathbf{2'}^{(3+)}$, remains essentially intact despite the rearrangement of monomeric parts in the process of the geometry optimization;[29] the O1···O2 and Ru1···Ru2 distances, 2.673 Å and 5.978 Å, respectively, are close to those determined in the solid state.[30]

From our calculations, it appears that the oxidation events, $\mathbf{2'}^{(3+)} \rightarrow \mathbf{2'}^{(4+)}$ and $\mathbf{2'}^{(4+)} \rightarrow \mathbf{2'}^{(5+)}$, are proton-coupled. Upon removal of an electron from $\mathbf{2'}^{(3+)}$ the $Ru2^{IV}O2H2^-$ unit readily transforms into $Ru^{IV}O^{\cdot}$ with the loss of a proton to solvent at the beginning of the geometry optimization of $\mathbf{2'}^{(4+)}$.[31] In the optimized structure of the $\{L(py)_2Ru^{IV}OH^{(-)}, {}^{\cdot}ORu^{IV}L(py)_2\}$ complex $\mathbf{2'}^{(4+)}$ (Figure 3), the hydrogen bond between the Ru1 bound OH group and solvent water is favored over the hydrogen bond between O1 and O2, as expected, since the Ru^{IV}-bound oxygen radical is a much weaker proton acceptor than a solvent water molecule. The removal of an electron from $\mathbf{2'}^{(4+)}$ initiates the proton-coupled formation of the second $Ru^{IV}O^{\cdot}$ fragment. The in-solvent optimized structure of the $\{L(py)_2Ru^{IV}O^{\cdot}, {}^{\cdot}ORu^{IV}L(py)_2\}^{5+}$ dimer ($\mathbf{2'}^{(5+)}$) is stable owing to the hydrogen-bonding network between opposing carboxylate groups.

A computation of the potential energy surfaces (PESs) of the evolution of the $\{L(py)_2Ru^{IV}O^{\cdot}, {}^{\cdot}ORu^{IV}L(py)_2\}^{5+}$ dimer ($\mathbf{2'}^{(5+)}$), which includes essential water molecules and three H_3O^+ ions, is far more challenging than the modeling of the preceding proton-coupled oxidation events. A main concern is the need for a computationally demanding equilibration of the explicit solvent for all points along the PESs. Since we have already demonstrated that "oxidation-coupled" protons are lost to solvent and taking into account the success of a SCRF-only description of solvent in previous studies of O_2 evolution through catalytic water oxidation,[17] we decided to proceed with a simplified dimer $\{L(py)_2Ru^{IV}O^{\cdot}, {}^{\cdot}ORu^{IV}L(py)_2\}^{2+}$ ($\mathbf{2''}^{(2+)}$), in SCRF-only solvent model. For calculations of PESs, it is intuitively reasonable to consider the O–O distance, r, as the reaction coordinate (see Figure 4). A large series of geometry optimizations of $\mathbf{2''}^{(2+)}$ with $r=3.9$–1.25 Å for all relevant spin configurations in SCRF was

 © 2010 Wiley-VCH Verlag GmbH & Co. KGaA, Weinheim

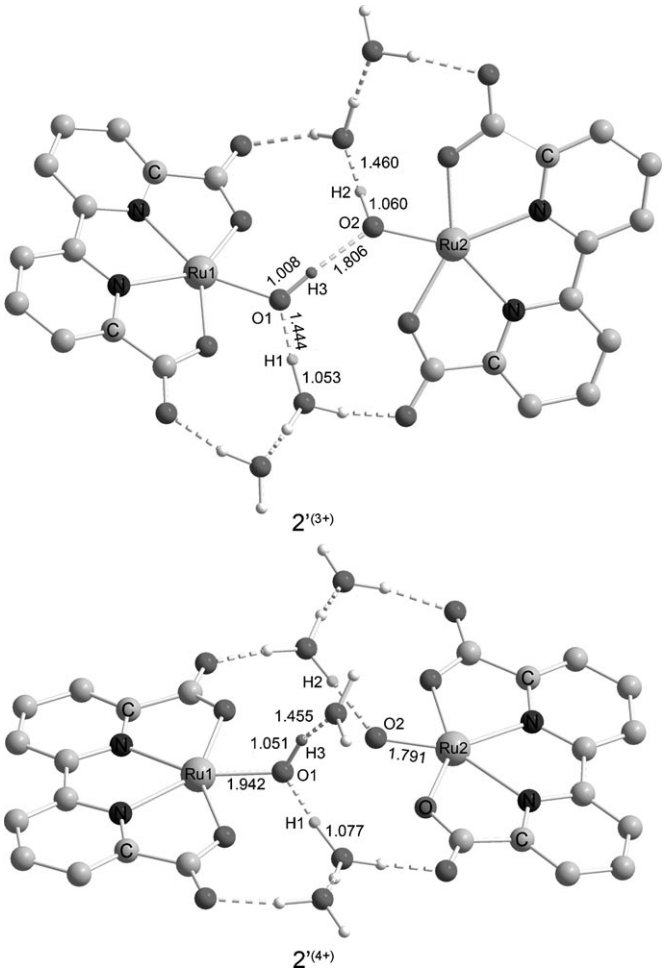

Figure 3. In-solvent optimized geometry of [μ-(HOHOH)-$\{Ru^{IV}L(py)_2\}_2]^{3+}$ ($\mathbf{2'^{(3+)}}$) and the $\{L(py)_2Ru^{IV}OH^-, {}^{\bullet}ORu^{IV}L(py)_2\}$ analogue ($\mathbf{2'^{(4+)}}$). Pyridine groups and additional water molecules are omitted for clarity. All distances are in Å.

Table 1: Selected Mulliken spin populations of the {RuO, ORu} fragment in $\{L(py)_2Ru^{IV}O^{\bullet}, {}^{\bullet}ORu^{IV}L(py)_2\}^{2+}$ dimer $\mathbf{2''^{(2+)}}$ versus O–O distance [Å] for two low-energy spin configurations.

O–O distance	Spin configuration	Ru1	O1	O2	Ru2
2.0	S(LS[AF])	0.2	0.7	−0.7	−0.2
	T(LS[F])	0.3	0.7	0.8	0.2
1.95	S(LS[AF])	0.1	0.8	−0.7	−0.1
	T(LS[F])	0.4	0.7	0.8	0.2
1.85	S(LS[AF])	0	0	0	0
	T(LS[F])	1.2	0.1	0.6	0.1
1.45	S(LS[AF])	0	0	0	0
	T(LS[F])	0.9	0.4	0.5	0.1

combined with the thorough analysis of possible conformers, as well as the molecular orbital (MO) analysis.

The low-energy electronic state of $\mathbf{2''^{(2+)}}$ features two unpaired electrons, one per $Ru^{IV}O^{\bullet}$ unit. The so-called low-spin antiferromagnetic, LS[AF], and the low-spin ferromagnetic, LS[F], configurations give rise to the most relevant low-energy singlet (S) and triplet (T) electronic states, respectively (Table 1). At an O–O distance larger than approximately 2.5 Å, these states are degenerate.[32]

As the O–O distance is decreased to approximately 2.0 Å in $\mathbf{2''^{(2+)}}$, the LS[AF] configuration becomes the most favorable, while the energy of the LS[F] configuration increases and remains greater than that of the LS[AF] configuration (see Figure 4). The potential-energy barriers for the direct O–O coupling are 12 kcal mol^{-1} and 15 kcal mol^{-1} for LS[AF] and LS[F] configurations, respectively (in SCRF). According to our calculations, the open-shell singlet (LS[AF]) and triplet (LS[F]) PESs lead to the peroxo, Ru^{IV}-$O_2^{(2-)}$-Ru^{IV}, and the superoxo, Ru^{III}-$^{\bullet}O_2$-Ru^{IV}, intermediates $\mathbf{3_S}$ and $\mathbf{3_T}$, respectively (Figure 4 and Figure 5). This has been also confirmed by independent geometry optimizations, starting from the structures of $\mathbf{2''^{(2+)}}$ with d(O–O) = 1.85 Å. The difference in energy between $\mathbf{3_S}$ and $\mathbf{3_T}$ is 8 kcal mol^{-1}. The O–O bond lengths in $\mathbf{3_S}$ and $\mathbf{3_T}$ are consistent with those for η^1:η^1 transition-metal complexes with peroxide (O_2^{2-}) and superoxide (O_2^{-}) anionic bridges, respectively.[33]

According to the MO analysis, the electronic structure of $\mathbf{3_S}$ features the doubly occupied σ2p bonding orbital, as well as two pairs of doubly occupied π2p/π*2p bonding/antibonding molecular orbitals of the O_2^{2-} fragment which bridges the d^4 Ru^{IV} centers, see also Mulliken spin populations in Table 1. The key features of the electronic structure of $\mathbf{3_T}$ is one partially occupied π*2p orbital of the superoxide bridge, O_2^{-}, and the apparent d^5 Ru^{III} center with one unpaired electron. The shorter O–O bond length in $\mathbf{3_T}$ than in $\mathbf{3_S}$ is the consequence of an additional two-center, three-electron bond between oxygen atoms (Figure 5).[34] Interestingly,

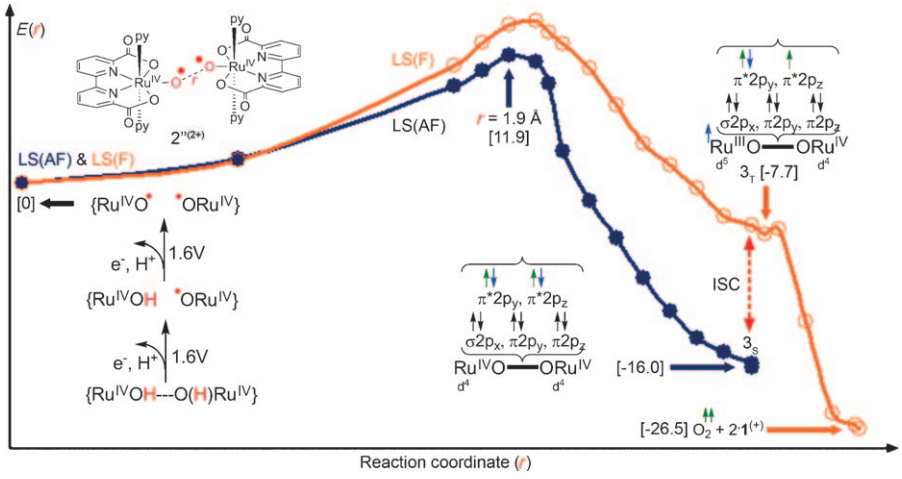

Figure 4. A direct pathway for evolution of O_2 in $\{L(py)_2Ru^{IV}O^{\bullet}, {}^{\bullet}ORu^{IV}L(py)_2\}^{2+}$ complex in SCRF (water), B3LYP/lacvp*. Potential energies in kcal mol^{-1} are shown in square brackets; σ1s/σ*1s and σ2s/σ*2s MOs of the O–O bridge are omitted for clarity; all O–O distances (r) are in Å.

© 2010 Wiley-VCH Verlag GmbH & Co. KGaA, Weinheim

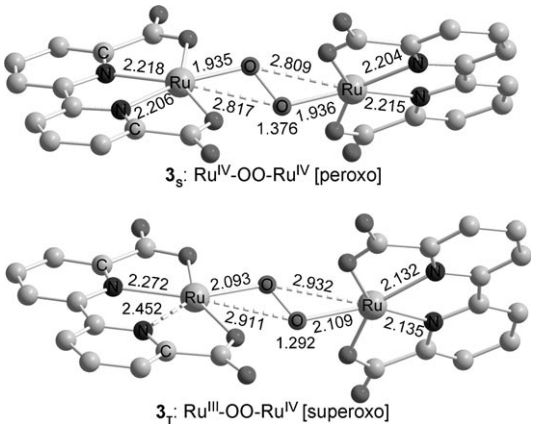

Figure 5. Optimized geometries of the peroxo and superoxo Ru-O_2-Ru complexes. Pyridine groups are omitted for clarity. All distances are in Å.

according to Mulliken spin populations, the so-called metal-to-metal charge transfer effects are very small in our case (Table 1).

Considering the small energy difference between $\mathbf{3_S}$ and $\mathbf{3_T}$, 8 kcal mol^{-1}, it is quite plausible that the intersystem crossing (ISC) between potential surfaces with different spin states takes place in a facile manner. While the peroxo intermediate is quite stable with regard to a perturbation of the O–O bond around the computed equilibrium, the superoxo intermediate is confined in a rather shallow potential well. A barrier of approximately 1.0 kcal mol^{-1} separates this intermediate from the dissociative region of the triplet potential-energy surface. Dissociation of a perturbed superoxo dimer into fragments: two Ru^{III} monomers, $\mathbf{1^{(+)}}$, and O_2, was verified computationally. According to Mulliken spin populations, the electron transfer from doubly occupied π*2p orbital of superoxide (O_2^-) to the Ru^{IV} center paves the way to the dissociation of Ru–O bonds in a perturbed superoxo ruthenium dimer. In this way the evolution of diradical O_2 is completed via the ISC between potential surfaces and subsequent rapid dissociation of $\mathbf{3_T}$.

In summary, we have accurately computed a binuclear pathway for the O_2 evolution, using a molecular model based on the well characterized Ru^{IV} complex **2**.[21] The key feature of our mechanism is that, first, the dissociation of O_2 from a peroxo intermediate does not require a high-energy ligand substitution, which was proposed by Yang and Baik in the computational study of Llobet's ruthenium Hbpp dimer (see Ref. [17b] and Ref. [11a], respectively); second, the computed reaction pathway does not lead to coordinatively unsaturated centers, such as the five-coordinate Ru^{II} in Ref. [17b]. Based on our calculations, we propose that the release of O_2 operates through two low-energy intramolecular electron transfers: first, $O_2^{2-} \rightarrow Ru^{IV}$, second, $O_2^- \rightarrow Ru^{IV}$. Computations by Yang and Baik predict barriers of approximately 14 kcal mol^{-1} and 31 kcal mol^{-1}, respectively, for the intramolecular O–O coupling towards a peroxo intermediate and the subsequent release of O_2.[17b] The latter appears to be in sharp disagreement with experimental study by Llobet et al., in which experimental evidence in favor of the intramolecular mechanism of O–O coupling is reported.[11a] In contrast, our results are consistent with Llobet's study, as well as the experimental results obtained in Ref. [21]. It is also noteworthy that our study portrays a catalytically active hydrogen-bonded dimer which does not have a direct coupling of the Ru centers by a common ligand framework; thus, a metal-to-metal charge transfer is much less pronounced in contrast with previously studied scenarios.

Received: November 15, 2009
Revised: December 12, 2009
Published online: February 12, 2010

Keywords: density functional calculations · O–O bond formation · redox chemistry · ruthenium

[1] T. J. Meyer, *Acc. Chem. Res.* **1989**, *22*, 163.
[2] T. J. Meyer, *Nature* **2008**, *451*, 778.
[3] P. E. M. Siegbahn, *Inorg. Chem.* **2008**, *47*, 1779.
[4] A. Kudo, H. Kato, I. Tsuji, *Chem. Lett.* **2004**, *33*, 1534.
[5] R. Eisenberg, H. Gray, *Inorg. Chem.* **2008**, *47*, 1697.
[6] V. Balzani, A. Credi, M. Vebturi, *ChemSusChem* **2008**, *1*, 26.
[7] L. Sun, L. Hammarström, B. Åkermark, S. Styring, *Chem. Soc. Rev.* **2001**, *30*, 36.
[8] J. H. Alstrum-Acevedo, M. K. Brennaman, T. J. Meyer, *Inorg. Chem.* **2005**, *44*, 6802.
[9] E. Amouyal, *Sol. Energy Mater. Sol. Cells* **1995**, *38*, 249.
[10] a) J. J. Concepcion, J. W. Jurss, J. L. Templeton, T. J. Meyer, *J. Am. Chem. Soc.* **2008**, *130*, 16462; b) C. W. Chronister, R. A. Binstead, J. Ni, T. J. Meyer, *Inorg. Chem.* **1997**, *36*, 3814; c) J. J. Concepcion, J. W. Jurss, J. L. Templeton, T. J. Meyer, *Proc. Natl. Acad. Sci. USA* **2008**, *105*, 17632; d) F. Liu, J. J. Concepcio, J. W. Jurss, T. Cardolaccia, J. L. Templeton, T. J. Meyer, *Inorg. Chem.* **2008**, *47*, 1727.
[11] a) S. Romain, F. Bozoglian, X. Sala, A. Llobet, *J. Am. Chem. Soc.* **2009**, *131*, 2768; b) X. Sala, I. Romero, M. Rodrguez, L. Escriche, A. Llobet, *Angew. Chem.* **2009**, *121*, 2882; *Angew. Chem. Int. Ed.* **2009**, *48*, 2842.
[12] a) J. K. Hurst, *Coord. Chem. Rev.* **2005**, *249*, 313; b) H. Yamada, W. F. Siems, T. Koike, J. K. Hurst, *J. Am. Chem. Soc.* **2004**, *126*, 9786.
[13] a) J. F. Hull, D. Balcells, J. D. Blakemore, C. D. Incarvito, O. Eisenstein, G. W. Brudvig, R. H. Crabtree, *J. Am. Chem. Soc.* **2009**, *131*, 8730; b) C. W. Cady, R. H. Crabtree, G. W. Brudvig, *Coord. Chem. Rev.* **2008**, *252*, 444.
[14] H.-W. Tseng, R. Zong, J. T. Muckerman, R. Thummel, *Inorg. Chem.* **2008**, *47*, 11763.
[15] J. Li, Y. Shiota, K. Yoshizawa, *J. Am. Chem. Soc.* **2009**, *131*, 13584.
[16] a) N. D. McDaniel, F. J. Coughlin, L. L. Tinker, S. Bernhard, *J. Am. Chem. Soc.* **2008**, *130*, 210; b) A. Sartorel, M. Carraro, G. Scorrano, R. D. Zorzi, S. Geremia, N. D. McDaniel, S. Bernhard, M. Bonchio, *J. Am. Chem. Soc.* **2008**, *130*, 5006.
[17] a) X. Yang, M.-H. Baik, *J. Am. Chem. Soc.* **2006**, *128*, 7476; b) X. Yang, M.-H. Baik, *J. Am. Chem. Soc.* **2008**, *130*, 16231.
[18] T. Privalov, L. Sun, B. Åkermark, J. Liu, Y. Gao, M. Wang, *Inorg. Chem.* **2007**, *46*, 7075.
[19] a) T. A. Betley, Q. Wu, T. Van Voorhis, D. G. Nocera, *Inorg. Chem.* **2008**, *47*, 1849; b) M. W. Kanan, D. G. Nocera, *Science* **2008**, *321*, 1072.
[20] a) J. T. Muckerman, D. E. Polyansky, T. Wada, K. Tanaka, E. Fujita, *Inorg. Chem.* **2008**, *47*, 1787; b) Y. V. Geletii, B. Botar, P. Kögerler, D. A. Hillesheim, D. G. Musaev, C. L. Hill, *Angew. Chem.* **2008**, *120*, 3960; *Angew. Chem. Int. Ed.* **2008**, *47*, 3896;

 © 2010 Wiley-VCH Verlag GmbH & Co. KGaA, Weinheim

c) C. S. Mullins, V. L. Pecoraro, *Coord. Chem. Rev.* **2008**, *252*, 416; d) Y. Xu, T. Åkermark, V. Gyollai, D. Zou, L. Eriksson, L. Duan, R. Zhang, B. Åkermark, L. Sun, *Inorg. Chem.* **2009**, *48*, 2717.

[21] L. Duan, A. Fischer, Y. Xu, L. Sun, *J. Am. Chem. Soc.* **2009**, *131*, 10397.

[22] A complete account of computational procedures and related references could be found in the Supporting Information. For all calculations, picoline groups are replaced by pyridine groups (py) for purely computational reasons.

[23] a) M. H. Baik, R. A. Friesner, *J. Phys. Chem. A* **2002**, *106*, 7407; b) L. E. Roy, E. Jakubikova, G. Guthrie, E. R. Batista, *J. Phys. Chem. A* **2009**, *113*, 6745; c) S. Blasco, I. Demachy, Y. Jean, A. Lledós, *New J. Chem.* **2001**, *25*, 611.

[24] H. Reiss, A. Heller, *J. Phys. Chem.* **1985**, *89*, 4207.

[25] a) M. H. V. Huynh, T. J. Meyer, *Chem. Rev.* **2007**, *107*, 5004; b) T. J. Meyer, M. Hang, V. Huynh, H. H. Thorp, *Angew. Chem.* **2007**, *119*, 5378; *Angew. Chem. Int. Ed.* **2007**, *46*, 5284.

[26] G. J. Tawa, I. A. Topol, S. K. Burt, R. A. Caldwell, A. A. Rashin, *J. Chem. Phys.* **1998**, *109*, 4852.

[27] M. Lundberg, M. R. A. Blomberg, P. E. M. Siegbahn, *Inorg. Chem.* **2004**, *43*, 264.

[28] Based on the benchmarks by Baik and Friesner (Ref. [23a]), the expected error of the potential reported herein is in the range of 0.26 V–0.38 V. See also reference [23b].

[29] The difference between the optimized in-solvent and solid-state structures of **2** is not surprising considering strong influence of packing interactions in the solid-state; a combination of π–π stacking between bipyridine units of L and edge–face CH–π interactions between picolines apparently influences the arrangement of aromatic moieties in the solid state of **2**, affording an alignment of Npic-Ru-Npic units; see also the Supporting Information.

[30] The in-solvent and gas-phase structures of **2** are quite similar; in the gas-phase structure the O···O and Ru···Ru distances are 2.541 Å and 5.858 Å, respectively.

[31] This could also be seen as the oxidation of Ru1 in concert with the shuffle of the proton between O1 and O2, which in turn is coupled with transfer of the proton, labeled as H2 in Figure 3, from the Ru2-$OH^{(-)}$ group to solvent.

[32] The difference between the potential energies of $\mathbf{2''}^{(2+)}$ complexes with the O–O distances of to 3.2 Å and 2.8 Å is only 0.24 kcal mol^{-1}. Considering optimized radii in Jaguar for O (1.6 Å), the zero-point of PESs in Figure 4 is set at an O–O distance of 3.0 Å.

[33] G. Q. Li, R. Govind, *Ind. Eng. Chem. Res.* **1994**, *33*, 755.

[34] a) L. Pauling, *The Nature of the Chemical Bond*, Cornell University Press, **1960**; b) M. Green, J. W. Linnet, *J. Chem. Soc.* **1960**, 4945; c) P. M. W. Gill, L. Radom, *J. Am. Chem. Soc.* **1988**, *110*, 4931.

 © 2010 Wiley-VCH Verlag GmbH & Co. KGaA, Weinheim